NANOSTRUCTURE AND BIOACTIVITY OF MOUSE LUNG EXTRACELLULAR MATRIX SCAFFOLDS

GARLIKOVA Zuzana[1,3], DUMKOVA Jana[1,4], ESNER Milan[1,3], RABATA Anas[1],
KOLEDOVA Zuzana[1], HAMPL Ales[1,2]

[1]Department of Histology and Embryology, Faculty of Medicine, Masaryk University, Brno,
Czech Republic, EU

[2]FNUSA-ICRC - International Clinical Research Center of St. Anne University Hospital Brno,
Czech Republic, EU

[3]CEITEC - Central European Institute for Technology, Masaryk University, Brno,
Czech Republic, EU

[4]Department of Animal Physiology and Immunology, Institute of Experimental Biology, Faculty of
Science, Masaryk University, Brno, Czech Republic, EU

Abstract

Extracellular matrix (ECM) forms an essential part of tissue microenvironment. Compositional and structural properties of ECM modulate behaviour of cells, including their differentiation, proliferation, and turnover. Here we aimed at detailed characterization of the nanostructure of lung ECM and evaluation of its bioactivity on cells grown *in vitro*. Mouse lungs were decellularized using 0.2 % sodium dodecyl sulphate, hypotonic solutions, and DNase. Morphological analysis of the resulting ECM scaffolds was performed by means of transmission and scanning electron microscopy. The ECM scaffolds retained 3D architecture of the main lung anatomical regions: the alveolar region and the blood/airway network. The region-specific ECM nanotopology and organization of ECM macromolecules such as fibres of collagen, elastin, and fibrillin were characterized. The lung ECM scaffolds were also homogenized and applied as a supplement to growth medium on primary lung cells *in vitro* to test the bioactivity of lung ECM. We demonstrate that homogenized ECM does not have a negative impact on the proliferation rate of primary lung cells. In conclusion, we herein show at nanoscale the morphological characteristics of lung ECM and demonstrate that lung ECM produced by decellularization procedure is compatible with *in vitro* cultured lung cells. These findings add to a better understanding of cells with their natural environment and can be valuable when designing applications of ECM for purposes in tissue engineering.

Keywords: Lung, extracellular matrix, nanostructure, bioactivity

1.   INTRODUCTION

Tissue engineering is a clinically driven field, that uses cells and natural or synthetic scaffolds to *in vitro* reconstruct tissues and/or whole organs to serve as an alternative to tissues/organs for transplantation [1]. Extracellular matrix (ECM) is a highly organized network of nanosized fibers of glycoproteins, proteins, and proteoglycans. ECM serves as a natural scaffold defining the shape and physical properties of tissues and organs. ECM also provides a niche-specific signaling to resident cells by immobilization of soluble growth factors and by exposing sequences for integrin binding. In epithelial tissue, a highly specialized form of ECM - the basal membrane is required to maintain epithelial cell polarity and directional movement of metabolic content [1]. *In vitro,* the natural ECM can be substituted with synthetic scaffolds in forms of nanofibers, gels, and/or foams, which are fine-tuned by means of their composition and structure [2]. Studies on synthetic scaffolds show that micro- and nanotopography of the scaffold are critical parameters, which affect cellular

processes such as cell adhesion [3,4], orientation [5], migration [3], and differentiation [5,6]. Therefore, to design scaffolds that will better mimic the ECM environment, complex knowledge of micro- and nanotopography of naturally occurring ECM is currently required. Decellularization is a method developed to remove cellular material from a particular tissue and/or organ, while leaving the ECM intact [7-11]. The result of tissue decellularization is an acellular 3D ECM scaffold, which maintains the original architecture of the tissue. In acellular ECM scaffolds, the nanostructure of the areas where cells are in a direct contact with ECM is exposed and can be visualized in detail by means of electron microscopy, unlike in non-decellularized tissues where the contact area is covered by continuous layer of cells. Here we decellularized mouse lung tissues and characterized micro- and nanotopology of ECM in alveolar, vascular, and airway regions of the lungs. The ECM scaffolds generated by decellularization of native lungs can be repopulated with cells *in vitro* and used as 3D tissue constructs for studying of cell-ECM interaction [7], for drug screening[12], and potentially also as transplants in clinic[13,14]. Here we investigated whether or not lung ECM influences behaviour of primary lung fibroblasts (LFs) cultured *in vitro* by assessing their cell proliferation. Our data evidence that proliferation of LFs is not dramatically affected by lung ECM added to the culture medium.
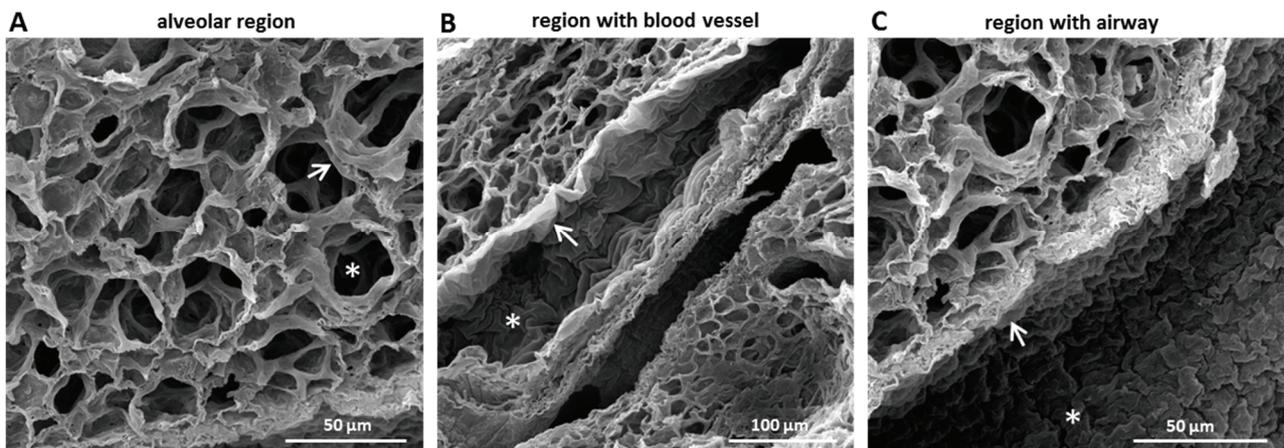
Figure 1 Microarchitecture of decellularized lungs

Representative images of alveolar region of decellularized lung tissues (A) with basal membrane of alveolar wall (white arrow) and alveolar space (white asterisk), as obtained by scanning electron microscopy. Image of decellularized blood vessel (B) showing denuded vascular wall (white arrow) and the lumen (white asterisk). Image of decellularized airway (C) showing denuded airway wall (white arrow) and airway lumen (white asterisk).

2. MATERIAL AND METHODS

2.1. Isolation and processing of lung ECM

Lungs were excised from mice (strain C57BL/6, 6-9 weeks of age), sectioned into cubic explants of approximately $2\,mm^3$ and then decellularized according to previously established protocol [15]. Shortly, the samples were embedded in OCT (Cryomatrix 6769006, Thermo Scientific) and underwent freeze/thaw cycle at -80°C. Subsequently the samples were incubated and agitated in hypotonic buffers, 0.2 % sodium dodecyl sulphate, DNase, followed by washes in PBS to remove cellular material. Resulting ECM scaffolds were processed for electron microscopy. For the use as medium supplement the samples were homogenized. ECM scaffolds were immersed in sterile PBS and mechanically disrupted by ceramic beads (MagNA Lyser Green Beads, Roche) using homogenizer (MagNA Lyser, Roche). Protein concentration was measured with DC

Assay according to the manufacturer's instructions (Bio-Rad). The homogenized ECM was passed through 0.22 μm filter to remove larger insoluble ECM particles. For each culture experiment fresh ECM was isolated and homogenized before application.

2.2.   Scanning electron microscopy of lung ECM scaffolds

Samples of decellularized lungs were fixed in 3 % glutaraldehyde in 100 mM cacodylate buffer for 2 h and then washed in cacodylate buffer (100 mmol/l sodium cacodylate in distilled water) for 15 min. The samples were dehydrated in 30, 50, 70, 80, and 96 % ethanol gradient (15 min per each concentration). The samples were dried at critical point dryer CPD 030 (Balzers Union Limited), sputtered with gold in a sputter coater SCD 030 (Balzers Union Limited), and observed on scanning electron microscope (Vega, Tescan).

2.3.   Transmission electron microscopy of lung ECM scaffolds

Samples of decellularized lungs were fixed in 3 % glutaraldehyde in 100 mM cacodylate buffer for 2 h and then washed in cacodylate buffer (100 mmol/l sodium cacodylate in distilled water) for 1 h. Samples were dehydrated in 70, 96, and 100 % ethanol gradient and then in 100 % acetone at 4°C, 40 min for each step. Subsequently, the samples were embedded in Durcupan resin. Ultrathin sections were prepared on ultramicrotome (LKB 8802A) and observed on transmission electron microscope (Morgagni 268D TEM, FEI).

2.4.   Isolation of mouse lung fibroblasts

Lungs from ICR mice (6-7 weeks old) were excised, washed with PBS and minced using scalpel. The sorting strategy was adapted from a previously published protocol [16]. For culture experiments primary lung fibroblasts from three independent isolations were used.

2.5.   Metabolic labelling with EdU and staining with DAPI

Cells were labelled with Click-iT^{TM} EdU Alexa Fluor 594 HCS Assay (Invitrogen) as follows: 20 μM EdU was added to culture medium for 1 h at 37°C and then the cells were fixed in 3.7 % formaldehyde for 15 min. Cells were permeabilized using 0.5 % Triton. Click-iT^{TM} reaction cocktail containing Alexa Fluor 549 azide was added and left for 30 min at room temperature, protected from light. Then the cells were washed off and remaining cell nuclei were stained with DAPI (Thermo Fisher Scientific, dilution 1:1000).

2.6.   Analysis of proliferation of lung fibroblasts cultured in medium supplemented by ECM

To study the effect of ECM contained in medium on cell proliferation, the LFs from three independent isolations were seeded in 96-well plate in density of 100 000 cells/well in medium (DMEM, 10 % FBS, 1x Insulin/Transferrin/Selenium, 0.5 % penicillin/streptomycin) supplemented with increasing concentration of homogenized ECM (0 ng/ml, 10 ng/ml, 1000 ng/ml). The cells were cultured for up to 72 h with change of medium every 24 h. The cells were taken for analysis (EdU, DAPI) at 24 h, 48 h, and 72 h, respectively. DAPI⁺ and EdU⁺ nuclei were detected using automatic high-throughput microscope (Image Express Micro, Molecular Devices). Image analysis was performed using software Cell profiler 2.4. Number of DAPI⁺ and EdU⁺ cells was calculated for each condition and expressed as mean ± SEM. The assay was performed using LFs from three independent isolations in technical triplicate.

The figure shows components of extracellular matrix of decellularized lungs as visualized by transmission electron microscopy (A-C). Image of alveolar region (A) with thin basal membrane (full arrowhead) separating the alveolar space (*Al*). Image of airway wall (B) showing basal membrane (full arrowhead) oriented towards the lumen of the airway (*L*), longitudinal section of collagen I fibers (full arrow) and transversal section of collagen I fibers (arrowhead), white area of elastin (asterisk) and fibers of fibrillin (arrow).
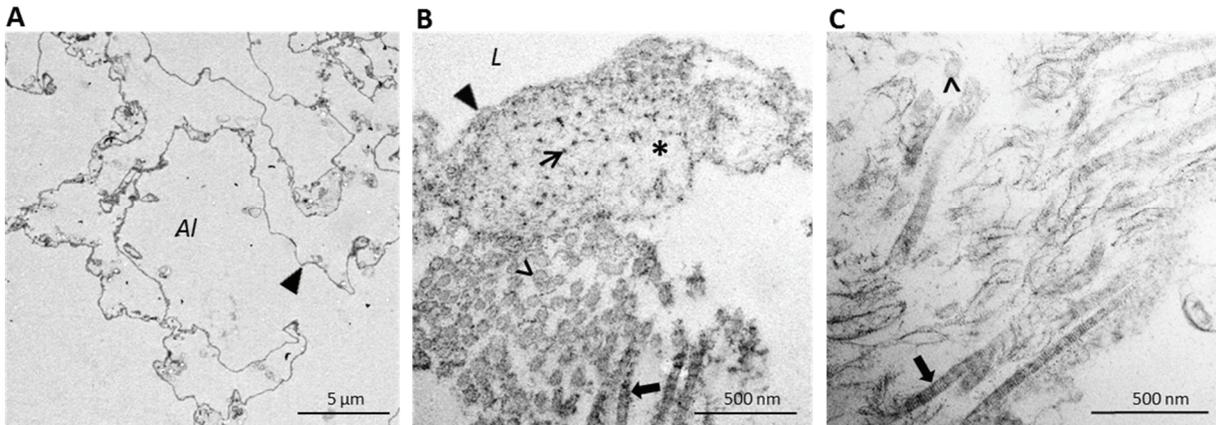
Figure 2 Nanoarchitecture of decellularized lung tissues

3. RESULTS

3.1. Morphology of lung ECM scaffolds
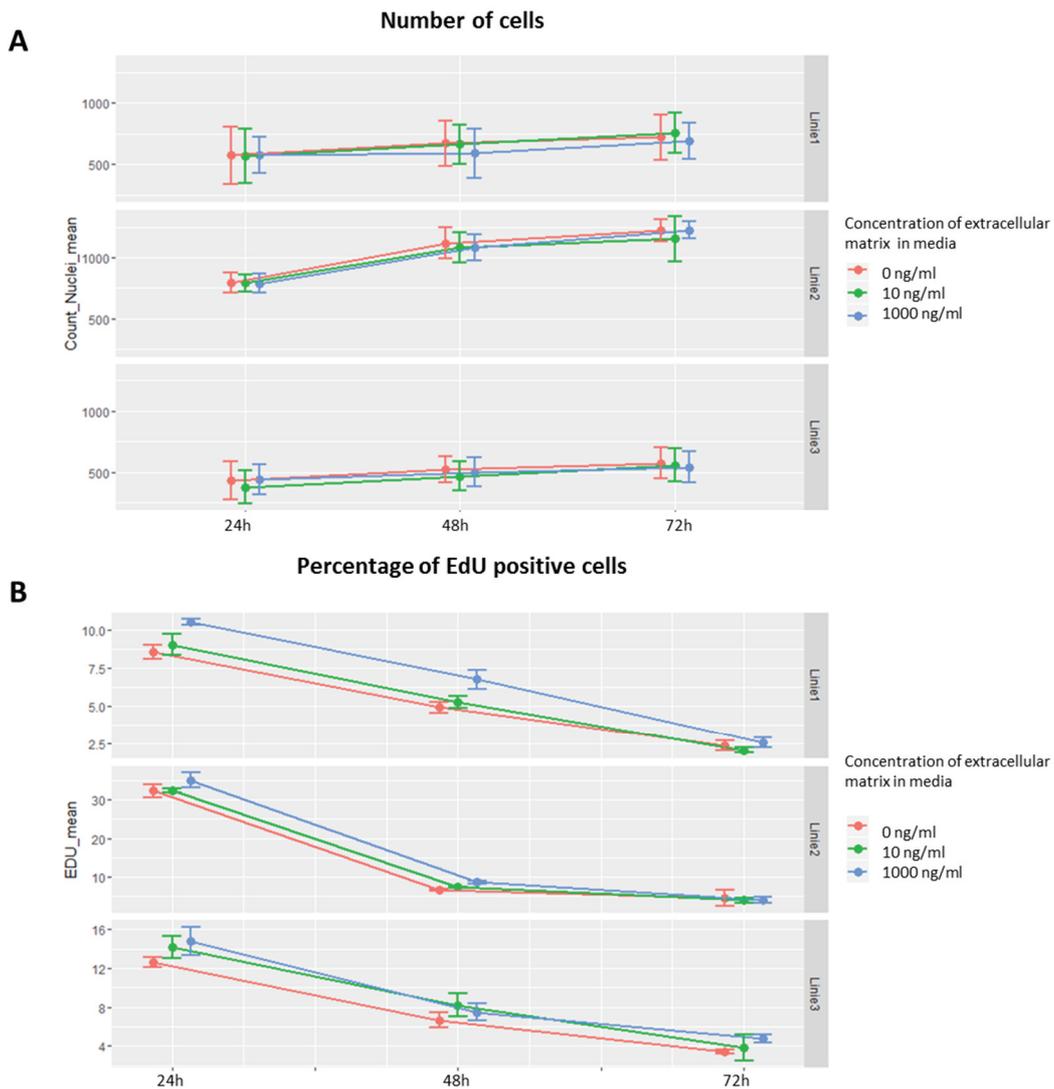
Figure 3 Effect of ECM contained in culture medium on proliferation of lung fibroblasts

Lung ECM scaffolds were devoid of cells and exhibited porous structure, in which blood vessels, airways, and alveoli were identified by means of scanning electron microscopy (**Figure 1**). In the alveolar region, thin basal membranes, oriented towards the alveolar spaces, were exposed (**Figure 1A**). Basal membranes were also observed to form inner layers of blood vessel walls (**Figure 1B**) and walls of airways (**Figure 1C**). Transmission electron microscopy images of lung ECM scaffolds showed, at nanoscale, the organization of the alveolar region (**Figure 2A**). Thin basal membranes, which in native lungs underlay a monolayer of epithelial cells, are exposed in ECM scaffold, separating individual alveoli (**Figure 2A**). Walls of airways are composed of intertwined bundles of elastin and fibrillin located underneath the basal lamina. Bundles of collagen I macromolecules are present throughout the walls, oriented to multiple directions as shown in **Figures 2B and 2C**.

Number of cell nuclei as determined over time of three days of culture of lung fibroblasts from three independent isolations in media supplemented with increasing concentrations of extracellular matrix (A). Percentage of proliferating cells, as determined by EdU positivity, over the time of 3 days of culture of lung fibroblasts from 3 independent isolations in media supplemented with increasing concentrations of extracellular matrix (B). Data are expressed as mean ± standard error of the mean.

3.2. Effect of ECM contained in culture medium on proliferation of LFs.

The similar growth of cells as determined by counting cell nuclei was evident in LFs from all three independent isolations irrespectively of the presence or absence (and concentration) of the ECM components in culture medum (**Figure 3A**). In other words, contents of ECM in culture medium did not influence growth of cells. We then determined the percentage of EdU$^+$ cells to determine number of cells in S-phase under the same conditions as described above. In all groups of LFs, the number of EdU$^+$ cells decreased over the time of 72 h in culture (**Figure 3B**). The content of ECM in culture medium affected slightly, however not significantly, the percentage of EdU$^+$ cells in all groups of LFs. We observed an increase in percentage of EdU$^+$ cells corresponding to increasing concentration of homogenized ECM in the medium. This effect was most pronounced at 24 h of culture and became diminished with the timely progression of culture. The increase in percentage of EdU$^+$ cells was not large enough to be significantly different when analyzed by two-tailed T-test.

4. DISCUSSION

Cells bind to the growth substrate via integrins, surface receptors, which upon binding activate cytoplasmic kinases, growth factor receptors, and control the organization of actin cytoskeleton. Also, in order for cells to proliferate, an integrin-mediated ECM anchorage is required [17,18]. Thus, the ECM exerts profound control over cells. Nanoscale surface topology of ECM directly influences integrin binding by defining the shape and area of the substrate to which the cells can attach [1]. In our work, we characterized the micro- and nanostructure of lung extracellular matrix by means electron microscopy. First, we decellularized mouse lungs in order to expose the ECM for visualization of the inner and superficial ECM structures. Along the alveolar and airway system the lungs are lined with epithelial cells attached to basal membranes - a specialized ECM structure consisting predominantly of collagens, laminins, and heparan sulphate proteoglycanes among other components [15]. In decellularized lungs we observed a typical porous structure of alveolar region consisting of network of thin basal membranes enclosing the alveolar spaces. The inner surface of the decellularized airways and blood vessels also consisted of relatively smooth layer of basal membrane. It was notable that the basal membrane in airways and blood vessels was creased. However, it is important to consider that the creasing could be a result of collaps of the airway and blood vessel walls during decellularization. Under the basal membranes of airway walls, we identified fibers of individual ECM macromolecules such as collagen I, fibrillin, and elastin, showing their spatial arrangement at nanoscale.

We then investigated if addition of homogenized ECM to growth media will affect proliferaltion of primary lung cells. We isolated LFs from mouse lungs and cultured them in ECM-supplemented medium. We show that

ECM contained in culture medium does not affect proliferation of LFs *in vitro*. We also show that in dose-dependent manner, the ECM in culture medium slightly, however not significantly, increases the percentage of cells in S-phase. This observation directs us to further investigation.

5. CONCLUSION

Our study shows morphology of micro- and nanostructures of lung ECM, characteristics, which can be translated to development of synthetic scaffolds for lung tissue engineering. Also, we show that lung ECM produced by decellularization is compatible with cells *in vitro*, as it does not negatively impact on proliferation of primary lung cells.

ACKNOWLEDGEMENTS

REFERENCES

[1]   C. ZHAO, A. TAN, G. PASTORIN, H.K. HO, Nanomaterial scaffolds for stem cell proliferation and differentiation in tissue engineering, Biotechnol. Adv. 31 (2013) 654-668. doi:10.1016/j.biotechadv.2012.08.001.

[2]   F. GELAIN, D. BOTTAI, A. VESCOVI, S. ZHANG, Designer self-assembling peptide nanofiber scaffolds for adult mouse neural stem cell 3-dimensional cultures, PloS One. 1 (2006) e119. doi:10.1371/journal.pone.0000119.

[3]   A. PALAIOLOGOU, D. STOUTE, Y. FAN, T.E. LALLIER, Altered cell motility and attachment with titanium surface modifications, J. Periodontol. 83 (2012) 90-100. doi:10.1902/jop.2011.100733.

[4]   X. WANG, X. HU, I. DULIŃSKA-MOLAK, N. KAWAZOE, Y. YANG, G. CHEN, Discriminating the Independent Influence of Cell Adhesion and Spreading Area on Stem Cell Fate Determination Using Micropatterned Surfaces, Sci. Rep. 6 (2016) 28708. doi:10.1038/srep28708.

[5]   G. ABAGNALE, M. STEGER, V.H. NGUYEN, N. HERSCH, A. SECHI, S. JOUSSEN, B. DENECKE, R. MERKEL, B. HOFFMANN, A. DRESER, U. SCHNAKENBERG, A. GILLNER, W. WAGNER, Surface topography enhances differentiation of mesenchymal stem cells towards osteogenic and adipogenic lineages, Biomaterials. 61 (2015) 316-326. doi:10.1016/j.biomaterials.2015.05.030.

[6]   X. WANG, S. LI, C. YAN, P. LIU, J. DING, Fabrication of RGD micro/nanopattern and corresponding study of stem cell differentiation, Nano Lett. 15 (2015) 1457-1467. doi:10.1021/nl5049862.

[7]   A.J. BOOTH, R. HADLEY, A.M. CORNETT, A.A. DREFFS, S.A. MATTHES, J.L. TSUI, K. WEISS, J.C. HOROWITZ, V.F. FIORE, T.H. BARKER, B.B. MOORE, F.J. MARTINEZ, L.E. NIKLASON, E.S. WHITE, Acellular Normal and Fibrotic Human Lung Matrices as a Culture System for In Vitro Investigation, Am. J. Respir. Crit. Care Med. 186 (2012) 866-876. doi:10.1164/rccm.201204-0754OC.

[8]   A.P. PRICE, L.M. GODIN, A. DOMEK, T. COTTER, J. D'CUNHA, D.A. TAYLOR, A. PANOSKALTSIS-MORTARI, Automated Decellularization of Intact, Human-Sized Lungs for Tissue Engineering, Tissue Eng. Part C Methods. 21 (2014) 94-103. doi:10.1089/ten.tec.2013.0756.

[9]   T.H. PETERSEN, E.A. CALLE, M.B. COLEHOUR, L.E. NIKLASON, Matrix Composition and Mechanics of Decellularized Lung Scaffolds, Cells Tissues Organs. 195 (2012) 222-231. doi:10.1159/000324896.

[10]   P.M. CRAPO, T.W. GILBERT, S.F. BADYLAK, An overview of tissue and whole organ decellularization processes, Biomaterials. 32 (2011) 3233-3243. doi:10.1016/j.biomaterials.2011.01.057.

[11]   S.L.M. DAHL, J. KOH, V. PRABHAKAR, L.E. NIKLASON, Decellularized native and engineered arterial scaffolds for transplantation, Cell Transplant. 12 (2003) 659-666.

[12]   D.E. WAGNER, N.R. BONENFANT, D. SOKOCEVIC, M.J. DESARNO, Z.D. BORG, C.S. PARSONS, E.M. BROOKS, J.J. PLATZ, Z.I. KHALPEY, D.M. HOGANSON, B. DENG, Y.W. LAM, R.A. OLDINSKI, T. ASHIKAGA, D.J. WEISS, Three-dimensional scaffolds of acellular human and porcine lungs for high throughput studies of lung disease and regeneration, Biomaterials. 35 (2014) 2664-2679. doi:10.1016/j.biomaterials.2013.11.078.

[13]   T. TSUCHIYA, A. SIVARAPATNA, K. ROCCO, A. NANASHIMA, T. NAGAYASU, L.E. NIKLASON, Future prospects for tissue engineered lung transplantation: decellularization and recellularization-based whole lung regeneration, Organogenesis. 10 (2014) 196-207. doi:10.4161/org.27846.

[14]   F.-M. CHEN, X. LIU, Advancing biomaterials of human origin for tissue engineering, Prog. Polym. Sci. 53 (2016) 86-168. doi:10.1016/j.progpolymsci.2015.02.004.

[15]   Z. GARLIKOVA, A.C. SILVA, A. RABATA, D. POTESIL, I. IHNATOVA, J. DUMKOVA, Z. KOLEDOVA, Z. ZDRAHAL, V. VINARSKY, A. HAMPLE, P. PINTO-DO-O, D.S. NASCIMENTO, GENERATION OF A CLOSE-TO-NATIVE IN VITRO SYSTEM TO STUDY LUNG CELLS-ECM CROSSTALK, Tissue Eng. Part C Methods. (2017).

[16]   J.L. MCQUALTER, K. YUEN, B. WILLIAMS, I. BERTONCELLO, Evidence of an epithelial stem/progenitor cell hierarchy in the adult mouse lung, Proc. Natl. Acad. Sci. U. S. A. 107 (2010) 1414-1419. doi:10.1073/pnas.0909207107.

[17]   F.G. GIANCOTTI, E. RUOSLAHTI, Integrin Signaling, Science. 285 (1999) 1028-1033. doi:10.1126/science.285.5430.1028.

[18]   C. GÉRARD, A. GOLDBETER, The balance between cell cycle arrest and cell proliferation: control by the extracellular matrix and by contact inhibition, Interface Focus. 4 (2014). doi:10.1098/rsfs.2013.0075.